

Quantum Approximate Optimization Algorithm in Non-Markovian Quantum Systems

Bo Yue and Shibe Xue*

1. *Department of Automation, Shanghai Jiao Tong University, Shanghai 200240, P. R. China*
2. *Key Laboratory of System Control and Information Processing, Ministry of Education of China, Shanghai 200240, P. R. China*
3. *Shanghai Engineering Research Center of Intelligent Control and Management, Shanghai 200240, P. R. China*

Yu Pan

4. *State Key Laboratory of Industrial Control Technology, Institute of Cyber-Systems and Control, College of Control Science and Engineering, Zhejiang University, Hangzhou 310027, P. R. China*

Min Jiang

5. *School of Electronics and Information Engineering, Soochow University, Suzhou 215006, P. R. China*

(Dated: August 4, 2022)

Quantum Approximate Optimization Algorithm(QAOA) is a promising quantum algorithm that can demonstrate quantum supremacy. The performance of QAOA on noisy intermediate-scale quantum (NISQ) devices degrades due to decoherence. In this paper, we present a framework for running QAOA on non-Markovian quantum systems which are represented by an augmented system model. In this model, a non-Markovian environment is modelled as an ancillary system driven by quantum white noises and the corresponding principal system is the computational unit for the algorithm. With this model, we mathematically formulate QAOA as piecewise control of the augmented system. To reduce the effect of non-Markovian decoherence, the above basic algorithm is modified for obtaining an efficient depth by a proximal gradient descent algorithm. Finally, in an example of the Max-Cut problem, we find non-Markovianity can help to achieve a good performance of QAOA, which is characterized by an exploration rate.

I. INTRODUCTION

Quantum computing has been a rapidly-growing technology since a polynomial-time quantum algorithm for large integer factorization [1, 2] and Grover algorithm for unstructured database searching [3] are proven to be exponentially accelerated compared to their classical counterparts. Although these quantum algorithms work for some specific problems, it has a long way to accelerate classical algorithms for some common problems such as combinatorial optimization problems which are NP-hard or even NP-complete.

In recent years, a class of quantum approximation optimization algorithms (QAOA) [4] is proposed for solving combinatorial optimization problems, which adopts a hybrid quantum-classical paradigm making use of a parameterized quantum circuit and a classical variational loop [5]. Instead of an optimal solution, QAOA can give an approximated solution in a short time. Initially, QAOA run on closed quantum systems, which was first applied to Max-Cut problem [4], and to Max E3LIN2 [6] soon after. Since Ref. [7] pointed out that QAOA can achieve so-called quantum supremacy, many advanced QAOAs were developed. Different from the above standard QAOA employing classical variational optimizers, Ref. [8] proposed a feedback-based strategy to

minimizing an optimization objective which has achieved fewer iterations than those in the standard one. Further, unconstrained QAOA was extended to solve combinatorial optimization problems with soft and hard constraints [9, 10]. To evaluate the performance of QAOA, a benchmark has been established in Ref. [11]. Also, many applications of QAOA were found. For example, QAOA were applied to generate non-trivial quantum states [12, 13], to solve the heterogeneous vehicle routing problem (HVRP) [14], the lattice protein folding problem [15], a clustering problem in unsupervised machine learning [16]. On the other hand, QAOA has been experimentally tested on small-scale quantum processors. In Ref. [17], QAOA was successfully run on two superconducting transmon qubits for the exact-cover problem. Also, in a two qubits system, Ref. [18] found that XY interactions can help to efficiently solve specific problems by reducing the depth of QAOA. Shortly afterwards, QAOA was run on a planar superconducting processor with 23 qubits for solving non-planar graph problems. Although the scaled processor involves noises and the problem is high-dimensional, the performance of QAOA was relatively robust, which put QAOA forward to practical applications [19]. With a long-range Ising model, the processor was scaled up to 40 trapped-ion qubits [20]. Although QAOA has been studied in various systems and problems, it presumes that the algorithm runs on a closed quantum system [4, 21–27], which limits its practical applications in principle.

* shbxue@sjtu.edu.cn

In the current stage of quantum computing, quantum information carriers are inevitably affected by decoherence and thus we have to run quantum algorithms on noisy intermediate-scale quantum (NISQ) devices [5, 28]. Correspondingly, how QAOA keeps its performance on NISQ devices is a research focus in recent years. Ref. [29] proposed an improved QAOA for Markovian quantum systems where control depth was minimized so as to reduce the influence of Markovian noises on the performance of the algorithm. Ref. [30] extended a rigorous analysis of the quantum optimal control problem to the open system setting and tested on both Quantum Annealing(QA) and QAOA. Different means harnessed to model Markovian quantum systems for QAOA, Ref. [31] used Pontryagin's minimum principle to optimize variational quantum algorithms for open quantum system with Markovian decoherence, [32] used an efficient Lagrangian-based approach to investigating an algorithm for quantum dynamics of the density matrix on NISQ devices, and [33] utilized deep quantum neural networks to represent the mixed states for open quantum many-body systems for QAOA. From a different perspective, Ref. [34] proposed a theory of learning nonlinear input-output maps with fading memory by dissipative quantum systems for Markovian QAOA. For a general picture, Ref. [35] gave Markovian models in quantum computing from a systematic review. However, when computational units are affected by more complicated noises, e.g., quantum colored noises [36–38], the units can exhibit totally different dynamics such that the performance of existing QAOAs degrades.

In this paper, we investigate QAOA for non-Markovian quantum systems which have been identified in solid-state quantum systems. To capture the dynamics of a non-Markovian quantum system with an arbitrary spectrum of quantum colored noises, we model the non-Markovian quantum system by an augmented system where an ancillary system represents the internal modes of the colored noises such that the spectrum of the fictitious output for the ancillary system is consistent with that of the non-Markovian environment. Also, the ancillary system is coupled to the computational units (principal system) by a direct interaction Hamiltonian such that the principal system undertakes non-Markovian dynamics. With this model, we first propose a framework for QAOA in non-Markovian quantum systems and then we improve it by optimizing the control depth of QAOA which achieves a balance between the performance of QAOA and the influence of the noises. Finally, numerical simulations on the Max-Cut problem show that QAOA in non-Markovian quantum systems can outperform that in Markovian quantum systems and a proper non-Markovianity can help to improve the performance of QAOA.

This paper is structured as follows. Section II provides a brief review of QAOA in close and Markovian open quantum system. QAOA in non-Markovian quantum systems is mathematically formulated in Section

III. In Section III C, we focus on optimizing the control depth of QAOA in non-Markovian quantum systems. Numerical simulations on the Max-Cut problem that tests the performance of our algorithm is presented in Section IV, where parameter analyses for the degree of non-Markovianity and comparisons the performance of QAOA between Markovian and non-Markovian quantum systems are conducted. Section V concludes our work.

II. BRIEF REVIEW OF QAOA IN QUANTUM SYSTEM FROM CLOSED TO OPEN

QAOA is a hybrid quantum-classical variational algorithm designed to tackle combinatorial optimization problems [21]. In this section, we briefly review noise-free(standard) QAOA in closed quantum systems, as well as noisy QAOA in Markovian quantum systems. We will first introduce how to convert a combinatorial optimization problem to a QAOA formulation and then give some basic notations in the algorithm.

A. Combinatorial optimization problems and Ising formulation

Combinatorial optimization is a kind of problems that searches solutions in a discrete but large space, which maximizes (or minimizes) an objective function. Typical examples entail Travelling Salesman problems, Knapsack problems and Max-Cut problems, etc. To deal with these problems, exhaustive search is not tractable, and only specialized algorithms that can quickly prune out useless solutions occupying large portion of search space and approximate algorithms are feasible at current situation.

To solve combinatorial optimization problems, Ising formulation is presented in Ref. [39], which can convert a classical objective function

$$\mathcal{V}(x_1, x_2, \dots, x_N) = - \sum_{i < j} J_{ij} x_i x_j + \sum_{i=1}^N h_i x_i, \quad (1)$$

into a quantum version Hamiltonian

$$H = \mathcal{V}(\sigma_1^z, \sigma_2^z, \dots, \sigma_N^z) = \sum_{\alpha=1}^M H_{\alpha}. \quad (2)$$

In Eq. (1), the objective involves n discrete variables $x_i \in \{-1, +1\}$, $i = 1, \dots, N$, where the parameters J_{ij} and h_i are real numbers. Since these variables take values identical to the eigenvalues of a spin system, we can replace x_i with the Pauli-z matrix σ_i^z and tensor the 2×2 identity matrix I for other spins beyond the replaced ones. For instance, when $N = 4$, a term $-J_{24}x_2x_4$ is converted into $-J_{24}I \otimes \sigma_2^z \otimes I \otimes \sigma_4^z$. Hence, N is also the total number of qubits in the algorithm, which equals to the logarithm of the number of solutions. In a specific problem, we can further write the Hamiltonian as

the summation of local cost functions H_α with the total number m . Here, we do not give the expression of H_α whose expression depends on the problem. In this way, the task of minimizing (maximizing) the classical objective is converted to find the minimum eigenvalue of the Hamiltonian H . For more details, see Ref. [39].

B. Standard QAOA in closed quantum systems

By far, many quantum algorithms that can potentially demonstrate the so-called quantum advantage are based on ideally universal fault-tolerant quantum computers with low error rates and long coherence durations [40]. In other words, the inherent quantum system has to be a closed quantum system; i.e., a quantum system does not exchange information with other systems. The state of a closed quantum system can be described by a wave function $|\psi(t)\rangle$. The time evolution of the state obeys Schrödinger equation $i\frac{\partial}{\partial t}|\psi(t)\rangle = H|\psi(t)\rangle$. Hereafter, we let Planck's constant \hbar to be 1. Alternatively, for a closed quantum system, its state can also be described by a density matrix $\rho(t) = |\psi(t)\rangle\langle\psi(t)|$ which satisfies Liouville-von Neumann equation

$$\dot{\rho}(t) = -i[H, \rho(t)], \quad (3)$$

where $[\cdot, \cdot]$ is the commutator of operators.

The standard QAOA encodes all possible solutions to a combinatorial optimization problem in quantum states. The objective function of the combinatorial optimization problem is also converted into a Hamiltonian H in quantum system as shown in the above subsection. QAOA intends to approach the ground state of H , which is an approximate solution closed to the optimal one [41]. Mathematically, the standard QAOA solves the following optimization problem

$$\min_{\tau=(\beta, \zeta)} f(\tau) = \min_{\tau=(\beta, \zeta)} \langle\psi(\tau)|H|\psi(\tau)\rangle, \quad (4)$$

where $f(\tau)$ is the expectation of H given $|\psi(\tau)\rangle$. Here, $\beta = (\beta_1, \dots, \beta_P)^T$ and $\zeta = (\zeta_1, \dots, \zeta_P)^T$ with the initial control depth of QAOA P are two vectors of durations for two unitary evolutions,

$$U(H, \zeta) = e^{-i\zeta H} = e^{-i\zeta \cdot \sum_{\alpha=1}^M H_\alpha} = \prod_{\alpha=1}^M e^{-i\zeta_\alpha H_\alpha}, \quad (5)$$

$$U(H', \beta) = e^{-i\beta H'} = e^{-i\beta \cdot \sum_{\theta=1}^N \sigma_\theta^x} = \prod_{\theta=1}^N e^{-i\beta_\theta \sigma_\theta^x}. \quad (6)$$

In terms of functionality, $U(H, \zeta)$ alters the phase of potentially good quantum states, while the mixing non-commuting Hamiltonian $H' = \sum_{\theta=1}^N \sigma_\theta^x$ enables the operator $U(H', \beta)$ to rotate quantum states to change the probability or weight of these good quantum states in superposition states. In addition, ζ and β , elements of ζ and β , are variational parameters that indicate control

durations of H and H' . Note that in the Hamiltonian H' the subscript θ in the Pauli-x matrix σ_θ^x indicates the order of qubits and thus we can further express it as $\sigma_\theta^x = I_1 \otimes \dots \otimes I_{\theta-1} \otimes \sigma_\theta^x \otimes I_{\theta+1} \otimes \dots \otimes I_n$ with 2×2 identity matrices I .

With the above notations, the standard QAOA can be described as follows. Initially, the state of qubits is prepared in a uniform superposition of all possible states $|\psi_0\rangle = |+\dots+\rangle = |+\rangle_n \dots |+\rangle_1$ with a superposition state $|+\rangle = \frac{1}{\sqrt{2}}(|0\rangle + |1\rangle)$ for the ground state $|0\rangle = (0, 1)^T$ and the excited state $|1\rangle = (1, 0)^T$. Further, the state of the qubits evolve as the master equation (3) where the Hamiltonian alternates between H and H' and the corresponding durations are determined by β and ζ , respectively. The above process can be described as

$$\rho_0 \xrightarrow{U(H, \zeta_1)} \rho_1 \xrightarrow{U(H', \beta_1)} \rho_2 \dots \xrightarrow{U(H, \zeta_p)} \rho_{2p-1} \xrightarrow{U(H', \beta_p)} \rho_{2p} \quad (7)$$

with $\rho_0 = |\psi_0\rangle\langle\psi_0|$, which is one iteration in QAOA. Here, we denote the state generated at the end of each iteration as $\rho(\tau) = \rho_{2p}$. The final state $\rho(\tau)$ is measured for several times and then the measurement results help to optimize the duration τ through an optimizer within a classical computer for the next iteration. Finally, with sufficient iterations, the state of qubits approaching to its ground state encodes an approximate optimal solution to the objective function of a combinatorial optimization problem.

C. Noisy QAOA in Markovian quantum systems

Since basically no quantum system is completely isolated from its environments and the quantum computers developed thus far have a limited coherence time. Hence, QAOA operating in a closed quantum system is far from reality. For noisy intermediate-scale quantum devices, it is necessary to consider QAOA in open quantum systems. An open quantum system interacts with an external environment or another quantum system, which significantly alters its dynamics and results in decoherence [42].

In open quantum systems, the performance of QAOA was first investigated in a class of Markovian quantum systems where the system is disturbed by flat spectrum quantum white noises [29]. Different from Eq. (3), the master equation

$$\dot{\rho}(t) = -i[H, \rho(t)] + \sum_{n=1}^N \gamma_n \mathcal{L}_{L_n}^*(\rho(t)), \quad (8)$$

for the density matrix $\rho(t)$ of a Markovian quantum system has an additional Lindblad term which characterizes the dissipation process in this system. Here, γ_n and L_n are the coupling strength and operator between each qubit and the environment for the n th dissipative channel. The Lindblad superoperator is calculated as $\mathcal{L}_{L_n}^*(\rho(t)) = \frac{1}{2}([L_n \rho(t), L_n^\dagger] + [L_n, \rho(t)] L_n^\dagger)$. For

more specifications concerning the modelling of Markovian quantum systems, see references [43–45].

Since the state of open quantum systems are described by a density matrix instead of a wave function, the optimization target for QAOA in Markovian quantum systems can be mathematically formulated as

$$\min_{\tau=(\beta,\zeta)} g(\tau) = \min_{\tau=(\beta,\zeta)} \text{tr}(H\rho(\tau)). \quad (9)$$

The basic procedure for QAOA in Markovian quantum systems is similar to that in closed quantum systems. However, due to the decoherence process, the system does not keep a unitary evolution. Hence, when we calculate the evolution of the state, we should use the master equation (8).

III. QAOA IN NON-MARKOVIAN QUANTUM SYSTEMS REPRESENTED BY AN AUGMENTED SYSTEM MODEL

Although Markovian quantum systems can capture parts of dynamics of open quantum systems, there exist other quantum systems involving complicated environments resulting in totally different dynamics from those of Markovian ones [46–49]. For example, non-Markovian quantum systems are disturbed by quantum colored noise generated by an environments with memory effects. Generally, the shape of the spectrum of a quantum colored noise $S(\omega)$ is not flat such that the system and environment can exchange information. This kind of non-Markovian quantum systems has been found in solid-state quantum systems such as quantum dots or superconducting systems [47]. To run QAOA in these solid-state systems, it is necessary to theoretically explore QAOA in non-Markovian quantum systems.

In this section, we will formulate QAOA in non-Markovian quantum system based on an augmented system model and give a corresponding basic algorithm. With respect to non-Markovian decoherence, we will also introduce an improved optimizer for QAOA where the depth of the algorithm can be reduced.

A. Augmented system model for non-Markovian quantum systems

As aforementioned, a non-Markovian environment is characterized by a noise spectrum $S(\omega)$ which indicates there exist internal modes in the environment. So an augmented system approach to representing a non-Markovian quantum system takes the dynamics of these internal modes of the non-Markovian environment into account such that we can describe the dynamics of the non-Markovian quantum system in an augmented Hilbert space [43].

In general, the shape of the spectrum of a non-Markovian environment can be arbitrary. When the

spectrum is rational, we can use quantum spectral factorization theorem to find a linear quantum system realization for the internal modes of the non-Markovian environment. Otherwise, Pade approximation method can be applied to approximate an irrational spectrum by a rational one such that we can also find its linear quantum system realization. In this way, we consider the linear quantum system realization for the non-Markovian environment as an ancillary system [43]. The ancillary system is actually a cluster of quantum harmonic oscillators. Its Hamiltonian is $H_a = \bar{a}^\dagger \Omega_a \bar{a}$ where \bar{a} is a vector of annihilation operators of the harmonic oscillators and Ω characterizes the internal energy of each oscillator as well as the interactions between them. These oscillators are driven by quantum white noise where their couplings are expressed by a vector of operators $L_a = N_a \bar{a}$ with a suitable dimensional matrix N_a describing the coupling strengths. To represent the quantum colored noise generated by the non-Markovian environment, a fictitious output is introduced $c_a = K_a \bar{a}$ with a suitable dimensional matrix K_a . Hence, we obtain the transfer function from the quantum white noise inputs to the fictitious output as $\Gamma(s) = -K_a (sI + i\Omega_a + \frac{1}{2}N_a^\dagger N_a)^{-1} N_a^\dagger$ where $s = -i\omega$ is the complex variable in Laplace transform. Note that quantum spectral factorization theorem for determining the corresponding matrices ω_a , K_a and N_a from a given spectrum $S(\omega)$ for the non-Markovian environment can be found in Ref. [43].

To capture the mutual influence between a non-Markovian system and its environment, an direct interaction Hamiltonian $H_{pa} = i(c_a^\dagger z - z^\dagger c_a)$ is introduced where z is a vector of operators for the non-Markovian system which is the principal system in the augmented system model. In such a way, supposing the original non-Markovian quantum system satisfies an integral-differential Langevin equation with a rational spectrum for the environment, this equation can be reproduced by that of the principal system in the augmented system model. This consistency enables us to represent the non-Markovian quantum system by the augmented system model [50].

In the Schrödinger picture, the augmented system model can be described by a master equation

$$\dot{\rho}(t) = -i[H_p + H_a + H_{pa}, \rho(t)] + \mathcal{L}_{L_a}^*(\rho(t)), \quad (10)$$

where $\rho(t)$ is the density matrix of the augmented system defined on the tensor space of the Hilbert space for the ancillary and principal systems. H_p is the Hamiltonian for the principal system, which will be found that this Hamiltonian describes the energy of qubits in QAOA. Note that although Eq. (10) is written in a Markovian form, the state of the principal system obey a non-Markovian dynamic, which can be obtained by tracing out the degree of freedom of the ancillary system from the density matrix of the augmented system model. Concretely, the density matrix of the principal system $\rho_p(t)$

can be calculated as

$$\rho_p(t) = \text{tr}_a(\rho(t)) = \sum_j \langle j|_a \rho(t) |j\rangle_a, \quad (11)$$

where tr_a is the partial trace with respect to the ancillary system and $|j\rangle_a$ is a set of orthogonal bases for the Hilbert space of the ancillary system.

B. Basic QAOA in non-Markovian quantum systems

With the augmented system model, we can design a QAOA in non-Markovian quantum system. Similar to the standard QAOA, the objective for QAOA in non-Markovian quantum systems is written as

$$\min_{\tau=(\beta,\zeta)} h(\tau) = \min_{\tau=(\beta,\zeta)} \text{tr}(H\rho_p(\tau)). \quad (12)$$

Note that we should use the density matrix for the principal system $\rho_p(\tau)$ to calculate the trace of the Hamiltonian but not that for the augmented system. However, the density matrix for the principal system $\rho_p(\tau)$ should be obtained from (11). Also, the alternative Hamiltonian control applies to the Hamiltonian of the principal system H_p .

The workflow of basic QAOA in non-Markovian quantum systems is described as follow. First, we randomly generate an initial duration vector τ_1 and the augmented system evolves with alternative Hamiltonians and relevant durations. Afterwards, the state of the principal system ρ_p and the corresponding objective $h(\tau_k)$ are calculated. Note that the classical optimizer in the basic algorithm is a gradient descent algorithm. Here, the gradient for the i -th segment of the duration vector τ is calculated as

$$[\nabla \text{tr}(H\rho_p(\tau))]_i = \frac{\text{tr}(H\rho_p(\tau_i + \epsilon)) - \text{tr}(H\rho_p(\tau_i - \epsilon))}{2\epsilon}, \quad (13)$$

where ϵ is a small positive perturbation. Consequently, τ_2 is updated along the gradient descent direction with a proper learning rate v . The above three steps repeats by multiple times until a terminating condition is satisfied which signifies the convergence of the objective $h(\tau)$. In the following algorithm, the terminating condition is chosen as the difference between two successive objectives and the threshold is denoted as η .

The specific algorithm of QAOA in non-Markovian quantum systems is detailed in Alg. 1.

Algorithm 1 Basic QAOA in non-Markovian quantum systems

Require: an initial duration vector τ_1 , a learning rate v , two Hamiltonians H, H' , a terminating threshold η

Ensure: the state of the principal system ρ_p and its corresponding objective $h(\tau_k)$

```

1:  $k = 1$ 
2: EVOLUTIONONCE( $\tau_k, H, H'$ )
3: do
4:    $k \leftarrow k + 1$ 
5:    $\tau_k = \tau_{k-1} - v \nabla \text{tr}(H \cdot \rho_p(\tau_{k-1}))$ 
6:   EVOLUTIONONCE( $\tau_k, H, H'$ )
7: while  $h(\tau_k) - h(\tau_{k-1}) < \eta$   $\triangleright$  terminating condition
8: return  $\rho_p, h(\tau_k)$ 
9:
10: function EVOLUTIONONCE( $\tau_k, H, H'$ )
11:    $p = \frac{1}{2} \|\tau_k\|$   $\triangleright \|\cdot\|$  denotes the vector length
12:   for  $j = 1, \dots, p$  do
13:      $\rho \leftarrow \hat{\rho} \leftarrow H_p = H$  in  $\beta_{jk}$  duration in Eq. (10)
14:      $\rho \leftarrow \hat{\rho} \leftarrow H_p = H'$  in  $\zeta_{jk}$  duration in Eq. (10)
15:   end for
16:  $\rho_p = \text{tr}_a[\rho]$   $\triangleright$  trace out ancillary system
17:  $h(\tau_k) = \text{tr}(H \cdot \rho_p)$ 
18: return  $h(\tau_k), \rho_p(\tau_k)$ 
19: end function

```

C. Optimizing depth for QAOA in non-Markovian quantum systems

Although we have designed the above QAOA in non-Markovian quantum systems, the performance of the algorithm would be degraded due to non-Markovian decoherence. One possible way to reduce the influence of non-Markovian decoherence on the performance is to squeeze the duration of our QAOA. Since the control depth p of $\tau = (\beta, \zeta)$ is an important indicator of the duration and space complexity of QAOA, we hope to lower the control depth p . Since parts of scattered values β and ζ would take small values which let the corresponding Hamiltonian H or H' lose their effects, we add l_1 norm of τ into the objective such that those β and ζ with small values can be diminished. Hence, the improved objective for the QAOA in non-Markovian quantum systems is written as

$$\min_{\tau=(\beta,\zeta)} y(\tau) = \min_{\tau=(\beta,\zeta)} \text{tr}(H\rho_p(\tau)) + \xi \|\tau\|_1, \quad (14)$$

where $\|\cdot\|_1$ refers to the l_1 norm and thus we have $\|\tau\|_1 = \sum_{\mu=1}^p (|\beta_\mu| + |\zeta_\mu|)$. The regularization parameter $\xi > 0$ indicates a balance between the result of QAOA and its calculation efficiency. It can be noted that p is not necessarily reduced since β_μ and ζ_μ is not necessarily punished to zero. However, a reduction of β_μ and ζ_μ is also important since this cuts down control duration which limits potentially the existing decoherence.

Traditional gradient descent method fails to find a solution to the optimization problem (14), as the l_1 regularization norm term is not differentiable. Hence, we adopt a proximal gradient (PG) descent algorithm to solve the

problem (14), which has been widely used in machine learning [51].

The major difference brought by PG descent algorithm is the soft-threshold operation, and the regularized QAOA in non-Markovian quantum systems is detailed in Alg. 2, where k is the current iteration step in Alg. 1.

Algorithm 2 Improved QAOA in non-Markovian quantum systems

Require: a duration vector τ_{k-1} , a learning rate v , a weight ξ , two Hamiltonians H, H' ,

Ensure: the updated duration τ_k , the state of the principal system ρ_p and its corresponding objective $h(\tau_k)$,

- 1: $y_k = \tau_{k-1} - v \nabla \text{tr}(H \rho_p(\tau_{k-1}))$
 - 2: $\tau_k = S_{\xi v}(y_k)$ ▷ soft-thresholding operation
 - 3: EVOLUTIONONCE(τ_k, H, H')
 - 4: **return** $\tau_k, \rho_p, h(\tau_k)$
-

The soft-threshold operation is defined as

$$S_{\xi v}([y_k]_i) = \begin{cases} [y_k]_i - \xi v, & [y_k]_i > \xi v \\ 0, & -\xi v \leq [y_k]_i \leq \xi v \\ [y_k]_i + \xi v, & [y_k]_i < -\xi v \end{cases} \quad (15)$$

The values of the control parameters are shifted towards zero by an amount of ξv . Furthermore, the parameter will be penalized to zero, if the condition $|[y_k]_i| \leq \xi v$ is fulfilled. By this means, less functional control parameters are eliminated, reducing the overall control depth. After a number of epochs of PG descent, $\hat{\tau}$ is obtained, and $\rho_p(\hat{\tau})$ gives solution to Eq. (14), and the approximate minimum value and corresponding solution to the combinatorial optimization problem can be obtained.

IV. NUMERICAL SIMULATIONS ON QAOA IN A NON-MARKOVIAN QUANTUM SYSTEM DISTURBED BY LORENTZIAN NOISE

To investigate the performance of our algorithm, we will give numerical results for QAOA in a non-Markovian quantum system with Lorentzian noise. In this section, we first introduce how we numerically simulate the dynamics of the non-Markovian quantum systems ;i.e., the master equation (10), to obtain the state of the principal system $\rho_p(\tau)$. Afterwards, the Max-Cut problem and the corresponding setup for the simulation are introduced. Further, we not only give our solutions to the Max-Cut problem but also explore how non-Markovianity affects the performance of our algorithm.

A. Numerical calculation of the dynamics of the augmented system model

For simplicity, we rewrite the master equation for the augmented system as

$$\dot{\rho}(t) = \mathcal{L}_0 \rho(t) \quad (16)$$

where the superoperator \mathcal{L}_0 is expressed as $\mathcal{L}_0 \rho(t) = -i[H_p + H_a + H_{pa}, \rho(t)] + \mathcal{L}_{L_a}^*(\rho(t))$. Since the master equation is time-invariant, its formal solution is expressed as

$$\dot{\rho}(t) = \exp\{\mathcal{L}_0(t - t_0)\} \rho(t_0). \quad (17)$$

In practical simulation, however, it is typically hard to obtain the analytical expression of Eq. (17), since it includes calculating the exponentials of the superoperator \mathcal{L}_0 . Instead, we discrete a total time T with a sampling time Δt and thus the density matrix at each sampling time $t_\chi = \chi \Delta t$ can be calculated as

$$\rho(t_\chi) = \mathcal{M}_\chi \mathcal{M}_{\chi-1} \cdots \mathcal{M}_1 \rho(t_0 = 0), \quad \chi = 1, 2, \dots, K, \quad (18)$$

where $\rho(t_0 = 0)$ is the initial density matrix of the system. The superoperator \mathcal{M}_κ is written as

$$\mathcal{M}_\kappa = \exp\{\Delta t \cdot \mathcal{L}_0\}, \quad \kappa = 1, 2, \dots, \chi, \quad (19)$$

which can be calculated through Taylor expansion. Finally, $\rho_p(\tau)$ can be obtained with Eq. (11). To obtain a precise result, we aggregate each Taylor expansion up to 20 terms in this paper.

B. Max-Cut and approximation ratio

The performance of QAOA in non-Markovian quantum systems is demonstrated on Max-Cut problem [6]. This problem is a classical combinatorial optimization problem and is known to be NP-complete. The problem considers an N -node undirected yet weighted graph $G = (V, E)$, where V is the node set and E is the edge set. Max-Cut is the partition of V into two subsets V_1 and V_2 , where the aggregation of weights of crossing edges is maximized. If we assign -1 to vertices in V_1 and 1 to vertices in V_2 , Max-Cut can be formulated as a binary optimization problem, vice versa. Namely, $C = \max \sum_{(i,j) \in E} \frac{\omega_{ij}}{2} (1 - s_i s_j)$, $s_i, s_j \in \{-1, +1\}$. For convenience, the equivalent form is used in this paper $C = \min \sum_{(i,j) \in E} \omega_{ij} s_i s_j$, $s_i, s_j \in \{-1, +1\}$, as the total weight is a constant. The corresponding Hamiltonian obtained from Ising formulation is

$$H = \sum_{(i,j) \in E} \omega_{ij} \sigma_i^z \sigma_j^z, \quad (20)$$

and we want to minimize the expectation of H as aforementioned. We use the approximation ratio

$$r = \frac{C_{max} - \text{tr}(H \rho_p(\hat{\tau}))}{C_{max} - C_{min}} \in [0, 1], \quad (21)$$

as a measure of how close the final state is to the optimal solution, where C_{max} and C_{min} are the theoretical maximum and minimum values of the original objective function, and $\rho_p(\tau)$ is the obtained final density matrix

by the algorithm. Obviously, the larger r , the better the solution indicated by the final state is. In this paper, we randomly generate an undirected yet weighted graph as depicted in the left graph of Fig. 1. In this graph, $C_{max} = 0.23 + 0.57 + 0.39 + 0.66 + 0.79 + 0.04 = 2.68$, where all the vertices are in the same group, while $C_{min} = -(0.57 + 0.39 + 0.66 + 0.79) + 0.23 + 0.04 = -2.14$, where the four vertices are partitioned into $\{1, 2\}$ and $\{3, 4\}$.

The experimental settings of our numerical simulations are given as follows. We conduct QAOA both in non-Markovian and Markovian quantum systems to demonstrate our strength. For non-Markovian quantum systems, we consider the principal system for QAOA is disturbed by Lorentzian noise generated from the ancillary system. The dimension of the ancillary system is truncated to be 8×8 . As a matter of fact, the dimension of the ancillary system should be higher than that of the principle system. In our instance, the principle system is comprised of 4 qubits, thus the dimension being $2^4 = 16$. By convention, the dimension of the ancillary system should be 20×20 or larger. However, we have tested the dimension from 8×8 to 20×20 and confirmed the output of QAOA and other numerical results are not influenced by the dimension of the ancillary system. Therefore, we reduce the dimension of the ancillary system to 8×8 to cut down computational and space complexity. The Hamiltonian of the ancillary system is $H_a = \omega_a a^\dagger a$, where the angular frequency of the ancillary system is $\omega_a = 10\text{GHz}$. The coupling operator $L_a = \sqrt{\gamma_0} a$, and $c = -\frac{\sqrt{\gamma_0}}{2} a$, where $\gamma_0 = 0.6$ is the damping rate of the ancillary system with regard to the quantum white noise field. Each qubit of the principal system is coupled with the ancillary system through the direct coupling operator $z = \sqrt{\kappa_1} \sigma_y$, with the coupling strength $\kappa_1 = 1\text{GHz}$. For Markovian quantum systems, the relaxation process in Markovian QAOA is simulated by $L_1 = \dots = L_4 = \sigma_-$, $\gamma_1 = \dots = \gamma_4 = 0.5$ in Eq. (8).

For the sake of intuition, we demonstrate the result of our Max-Cut instance in Fig. 1. In our notation, $|0\rangle$ and $|1\rangle$ are used to specify the group where each of the four vertices is in. For example, $|0011\rangle$ means vertex 1 and 2 are in the same group labeled by $|0\rangle$, while vertex 3 and 4 are in the other group $|1\rangle$. Remarkably, $|1100\rangle$ outputs the same result as $|0011\rangle$, since the objective function simply calculates the aggregated weights of the crossing edges. As mentioned above, QAOA raises the possibilities of good solutions, and these potentially optimal solutions will always be collapsed into when enough measurements are taken in quantum devices. We illustrate the possibility of each possible solution in Fig. 2. The optimal solution $|1100\rangle$ or $|0011\rangle$ accounts for 0.8260 in 1, which is the largest among eight possible solutions. The corresponding value of the optimal solution is -2.14 , which equals to C_{min} . Although both Markovian QAOA and non-Markovian QAOA gives the maximum possibility to the optimal solution in our experiment, advantages of non-Markovian QAOA over Markovian QAOA

is illustrated in Fig. 2, where the aggregated possibilities of good enough solutions (the first three) of non-Markovian QAOA (0.8629) far outweigh that of Markovian QAOA (0.7155).

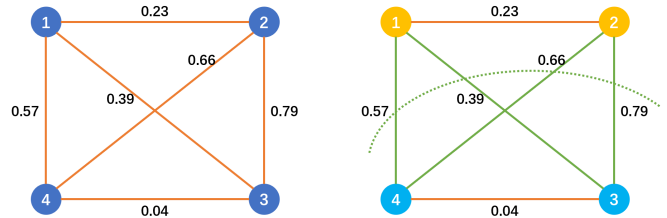


FIG. 1. The left graph is the undirected and weighted graph which is randomly generated and is applied in simulation. The graph is a regular graph composed of 4 nodes and 6 differently-weighted edges. The right graph is the result of our Max-Cut instance. The 4 green edges are the crossing edges, and the dotted green curve is the max-cut (solution), which partitions the nodes into two categories (yellow and blue).

C. Performance comparison between initialized and improved QAOA in the non-Markovian quantum system

We show the performance comparison between the initialized and improved QAOA in the non-Markovian quantum system with quantum Lorentzian noise in Fig. 3. In this figure, approximation ratios with different initial depth from $p = 1$ to 4 are depicted. Due to the optimization achieved by the PG descent algorithm, the improved QAOA outperforms the initialized QAOA in the non-Markovian quantum system by $0.2 \sim 0.3$ in r .

Although increasing the control depth p leads to a performance improvement in general, the degree of improvement is relatively subtle after $p = 2$. On one hand, the noise effect accumulates along with the growth of p . On the other hand, as increasing the number of the control parameters, the computational burden grows. Hence, there exists a trade-off between the performance and the cost of QAOA which includes time and space complexity and increasing efforts spent on restraining noise effects, as p grows. Apparently, we intend to select $p = 2$ for our instance, which achieves 0.9244 in r and has relatively cost in the operation of QAOA. The corresponding optimized control parameters for $p = 1, 2, 3, 4$ are $[2.0, 0.6]$, $[2.1, 0.5, 2.1, 1.9]$, $[2.1, 0.5, 1.6, 1.4, 0.4, 2.0]$, $[1.4, 0.6, 1.6, 0.5, 0.9, 0.4, 1.4, 0.5]$, respectively.

D. How non-Markovianity affects the performance of QAOA

Next, we investigate how non-Markovianity affects the performance of QAOA. The definition of the measure of

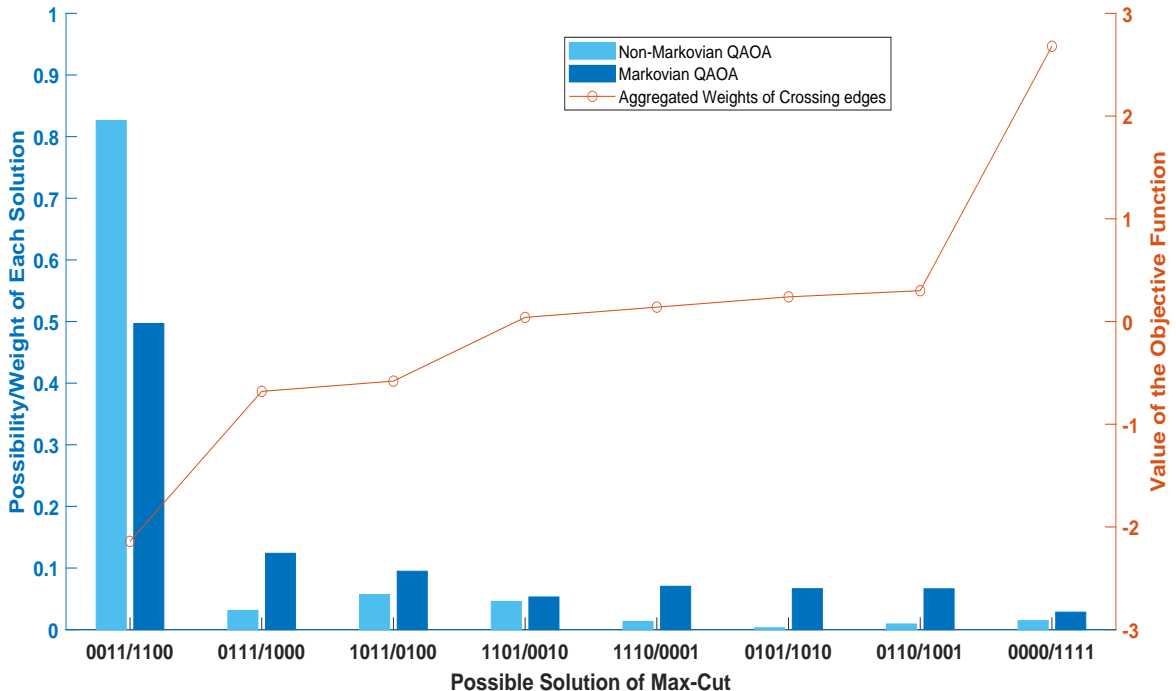


FIG. 2. The possibility and value of each of the 8 possible solutions in non-Markovian QAOA and Markovian QAOA. The bar chart follows the left y axis, while line chart follows the right y axis. The left y axis shows the possibility or weight of each solution in the final superpositioned quantum state, while the right y axis shows the corresponding objective value for each solution, which is obviously the same for both non-Markovian and Markovian QAOA. The light blue bar chart depicts non-Markovian QAOA, while the dark blue bar chart depicts Markovian QAOA. Both non-Markovian QAOA and Markovian QAOA are optimized based on initial depth $p = 2$ and all control parameters initialized as 3. As for the optimal solution, the weight in non-Markovian QAOA is 0.8260 given $(\zeta_1, \beta_1, \zeta_2, \beta_2) = (2.1, 0.5, 2.1, 1.9)$, while the weight in Markovian QAOA is 0.4968 given $(\zeta_1, \beta_1, \zeta_2, \beta_2) = (0.5, 1.0, 0.9, 1.2)$. Clearly, non-Markovian QAOA performs much better than Markovian QAOA.

non-Markovianity in our quantum process is given and then we discuss the detailed impact of non-Markovianity on the performance of QAOA.

1. Measure for the degree of non-Markovianity

In this paper, we adopt the measure for the degree of non-Markovian behavior in open quantum systems constructed in Ref. [52]. The essential property of non-Markovianity is the growth of distinguishability between two quantum states under quantum evolution, which can be interpreted as a flow of information from the environment back to the open system. The measure in Ref. [52] is based on the trace distance of two quantum states

$$D(\rho_1, \rho_2) = \frac{1}{2} \text{tr} |\rho_1 - \rho_2|, \quad (22)$$

describing the probability of successfully distinguishing the two states, where ρ_1 and ρ_2 are two time-evolving density matrices of a pre-defined quantum processes, and $|A| = \sqrt{A^\dagger A}$ for an arbitrary operator A . Further, the rate of change of the trace distance for a given quantum

process $\Phi(t)$ is defined by

$$\sigma(t, \rho_{1,2}(0)) = \frac{d}{dt} D(\rho_1(t), \rho_2(t)), \quad (23)$$

where $\rho_{1,2}(0)$ are the initial states of ρ_1 and ρ_2 . Obviously, $\sigma \leq 0$ throughout any non-Markovian quantum process. Naturally, the measure $\mathcal{N}(\Phi)$ for the non-Markovianity of the quantum process $\Phi(t)$ is defined by

$$\mathcal{N}(\Phi) = \max_{\rho_{1,2}(0)} \int_{\sigma > 0} dt \sigma(t, \rho_{1,2}(0)). \quad (24)$$

If we define (t_i, t'_i) as the time interval where σ is positive, Eq. (24) can be converted into

$$\mathcal{N}(\Phi) = \max_{\rho_{1,2}(0)} \sum_i [D(\rho_1(t'_i), \rho_2(t'_i)) - D(\rho_1(t_i), \rho_2(t_i))]. \quad (25)$$

In order to calculate $\mathcal{N}(\Phi)$ in practice, we first figures out any pair of initial states and the aggregated growth of trace distance over each time interval (t_i, t'_i) . Then, we determine the maximum over all potential pairs of the initial states.

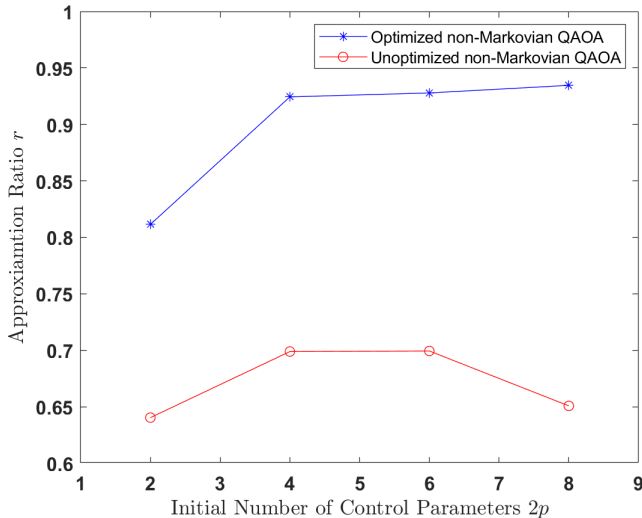


FIG. 3. The performance comparison between the initialized and improved QAOA in the non-Markovian quantum system with different number of control parameters. When $p = 1$, there are 2 control parameters, the performance is not good enough. When $p \geq 2$, the approximation ratio are 0.9244, 0.9279, and 0.9346, respectively, which is already sufficient for a good solution, and indicates a large weight of optimal solution in the final superposition quantum state.

2. Non-Markovianity and Performance of QAOA varying with three parameters in the augmented system model

In our augmented system model, the non-Markovian environment is parameterized by the ancillary system. To investigate the relation between non-Markovianity and the performance of QAOA, we specify the spectrum of the non-Markovian environment as a Lorentzian spectrum

$$S_0(\omega) = \frac{\frac{\gamma_0^2}{4}}{\frac{\gamma_0^2}{4} + (\omega - \omega_a)^2}, \quad (26)$$

where ω_a and γ_0 determine the center and the width of the spectrum. This environment is represented by a one-mode oscillator in the augmented system model, where ω_a and γ_0 are the angular frequency and the damping rate to quantum white noise of the oscillator, respectively [43]. Also, the coupling strength κ_1 determines the amplitude of the spectrum [43]. In addition, to calculate the non-Markovianity of the system for QAOA, we choose the state of the principal system as $\rho_1(0) = |+\rangle^n \langle +|^n$ and $\rho_2(0) = |-\rangle^n \langle -|^n$ to maximize the sum of the growth of D as suggested in Ref. [52]. Hence, in the following we will observe how these parameters vary the non-Markovianity of the system of interest $\mathcal{N}(\Phi)$ and the performance of QAOA r such that we try to establish the relation between the non-Markovianity and the performance of QAOA. The initialized control parameters are randomly selected, while the optimized control param-

eters are obtained via Alg. 2.

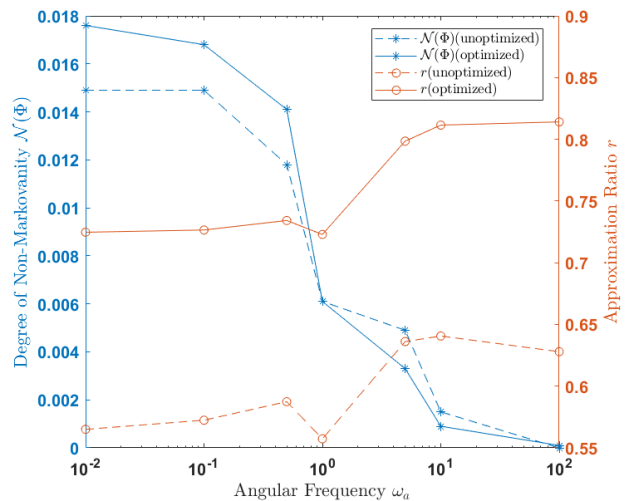


FIG. 4. The influence of ω_a on $\mathcal{N}(\Phi)$ and r . The dashed line is obtained by unoptimized control parameters, which is initialized as 3, and $p = 1$, while the solid line is obtained by optimized control parameters which varies at each point. The blue line is the curve of $\mathcal{N}(\Phi)$, while the red line is the curve of r . The axis of ω_a is of logarithmic coordinates for larger range. On average, the PG algorithm raises the performance of QAOA by 0.2 in r .

The influence of ω_a on $\mathcal{N}(\Phi)$ The non-Markovianity $\mathcal{N}(\Phi)$ varying with the frequency ω_a is plotted in Fig. 4. The dashed and solid lines indicate the control parameters are not optimized and optimized by the PG algorithm, respectively. The blue line describes the variation of the non-Markovianity $\mathcal{N}(\Phi)$, while the red line represents the performance of QAOA r . From the figure, we find the non-Markovianity $\mathcal{N}(\Phi)$ reaches its peak when the principal system resonates with the ancillary system. In this case, the principal system is significantly disturbed by the ancillary system. When $\omega_a < 1$, $\mathcal{N}(\Phi)$ with optimized control parameters is larger than $\mathcal{N}(\Phi)$ with initialized control parameters. As ω_a grows, r also grows, which gives us a hint to achieving better result of QAOA that ω_a had better be larger than 10.

The influence of κ_1 on $\mathcal{N}(\Phi)$ We plot the non-Markovianity $\mathcal{N}(\Phi)$ varying with the coupling strength κ_1 in Fig. 5, where $\mathcal{N}(\Phi)$ increases monotonically with κ_1 . This is because a large κ_1 means the coupling strength between the principal system and the ancillary system is large, which means a large $\mathcal{N}(\Phi)$. This indicates κ_1 is a major influencing factor of $\mathcal{N}(\Phi)$. When $\kappa_1 < 5$, $\mathcal{N}(\Phi)$ with optimized control parameters is larger than $\mathcal{N}(\Phi)$ with initialized control parameters. The performance of QAOA indicated by r decreases monotonically with κ_1 , as the QAOA system is increasingly disturbed by the ancillary system with the growth of κ_1 . As κ_1 grows, r decreases, which gives us a hint to achieving better result of QAOA that κ_1 had better be

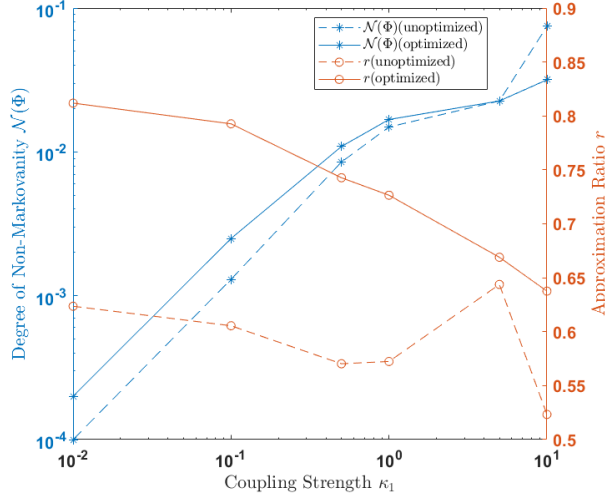


FIG. 5. The influence of κ_1 on $\mathcal{N}(\Phi)$ and r . The dashed line is obtained by unoptimized control parameters, which is initialized as 3, and $p = 1$, while the solid line is obtained by optimized control parameters which varies at each point. The blue line is the curve of $\mathcal{N}(\Phi)$, while the red line is the curve of r . The axis of κ_1 and $\mathcal{N}(\Phi)$ is of logarithmic coordinates for larger range.

smaller than 0.1.

The influence of γ_0 on $\mathcal{N}(\Phi)$ We demonstrate this influence in Fig. 6. $\mathcal{N}(\Phi)$ first increases with γ_0 , and reaches its peak at $\gamma_0 = 1$, and then decreases with γ_0 . This is due to the Lorentzian power spectral density of the form [43] where ω_a is the angular frequency of the ancillary system. It is clear that when γ_0 approaches 0 or $+\infty$, the Lorentzian noise reduces into the white noise, and the principal system becomes a Markovian system, causing $\mathcal{N}(\Phi)$ to approach 0. The performance of QAOA denoted by r decreases monotonically when $\gamma_0 \geq 1$, since a large γ_0 could lead to quantum decoherence, which lowers r . When $0 < \gamma_0 < 1$, r is irrelevant of γ_0 . This also offers us a hint to achieving better result of QAOA that γ_0 had better be kept under 1.

The influence of $\mathcal{N}(\Phi)$ on the approximation ratio r As aforementioned, the essential property of the non-Markovian behavior is the growth of distinguishability between quantum states. A large value of $\mathcal{N}(\Phi)$ indicates the fact that the density matrix tends to vary drastically, thus exploring the potential solutions represented by quantum states more completely. Nonetheless, if $\mathcal{N}(\Phi)$ exceeds a certain amount, the exploration process becomes too fast to converge to a good enough solution, leading to a low r . This resembles the idea “balance between exploration and exploitation” in Reinforcement Learning [53]. Only if both exploration and exploitation are properly taken into account can we obtain a good result. In our paper, the evolution of QAOA is responsible for exploration and PG algorithm accounts for exploitation. Thus, a proper exploration procedure is preferred.

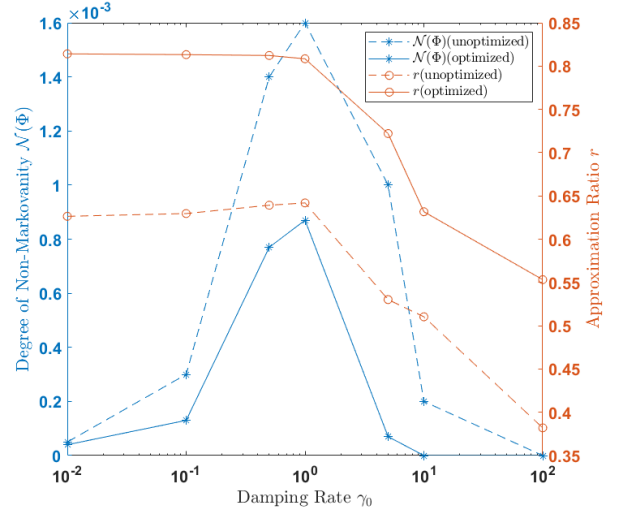


FIG. 6. The influence of γ_0 on $\mathcal{N}(\Phi)$ and r . The dashed line is obtained by unoptimized control parameters, which is initialized as 3, and $p = 1$, while the solid line is obtained by optimized control parameters which varies at each point. The blue line is the curve of $\mathcal{N}(\Phi)$, while the red line is the curve of r . The axis of γ_0 is of logarithmic coordinates for larger range.

In other words, if the principal system under current control parameters fail to offer a good solution as expected, altering control parameters towards the direction that increases $\mathcal{N}(\Phi)$ is a good option. Hence, selected parameters, including both control parameters and experimental settings should provide a moderate $\mathcal{N}(\Phi)$, typically around 10^{-3} , so as to achieve a good r .

In order to better characterize the significance of exploration on the approximation ratio r , we define

$$\bar{\sigma}(\Phi) = \frac{\mathcal{N}(\Phi)}{T} \quad (27)$$

as the exploration rate, which signifies the average degree of exploring quantum states in a quantum process $\Phi(t)$, and T denotes the total amount of time spent for $\Phi(t)$. We randomly select 25 groups of control parameters, and obtain corresponding $\bar{\sigma}(\Phi)$ and r , depicted in Fig. 7. Clearly, when $\bar{\sigma}(\Phi) < 2 \times 10^{-3}$, the exploration is far from enough that a good solution is hardly detected. When $\bar{\sigma}(\Phi)$ is between 2×10^{-3} and 4×10^{-3} , we consider the exploration of good solutions is relatively sufficient. However, when $\bar{\sigma}(\Phi)$ continues to grow above 4×10^{-3} , the step for exploration becomes so large that good solutions can be skipped. The filled upside triangle denotes a quantum process that is more sensitive to $\bar{\sigma}(\Phi)$, and can find a relatively good solution even when $\bar{\sigma}(\Phi)$ is not large enough. On the contrary, the filled downside triangle denotes a quantum process that is not sensitive to $\bar{\sigma}(\Phi)$, and is able to find a relatively good solution even when $\bar{\sigma}(\Phi)$ is large. We use green dashed lines to denote the upper bound and lower bound of points. So we can clearly see a tradeoff for exploration rate here. To

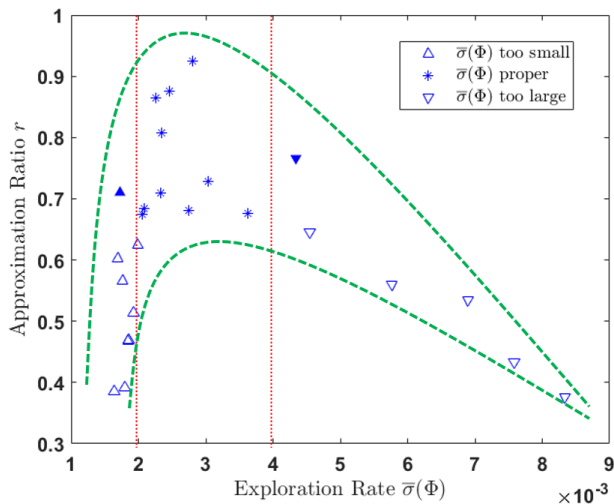


FIG. 7. The influence of $\bar{\sigma}(\Phi)$ on r . The experiment is conducted under the condition that $p = 2$, and τ is randomly selected between 0.5 and 4. Since $\bar{\sigma}(\Phi)$ is measured after the evolution of a quantum process, we can only use scatter plots to demonstrate our results. The green dashed lines denotes the upper bound and lower bound of points. So we can clearly see a tradeoff for exploration rate here.

sum up, a proper exploration rate contributes to the performance of QAOA, and can serve as a guidance when

optimizing control parameters.

V. CONCLUSION

In our work, we have presented an augmented system model framework for QAOA in non-Markovian quantum systems. Following the standard QAOA, we proposed a basic QAOA in non-Markovian quantum systems. To reduce the influence of non-Markovian decoherence on the performance of QAOA, we also improved the basic algorithm by introducing an l_1 regularization term which can reduce the depth of our algorithm. The effectiveness of the above algorithms are verified in an example of the Max-Cut problem, where the algorithms run in a non-Markovian quantum system disturbed by Lorentzian noise. Our algorithm can achieve a better performance than that in Markovian quantum systems. Importantly, we find a proper non-Markovianity can help to obtain a better result. Hence, we need to carefully choose parameters of non-Markovian quantum systems to guarantee non-Markovianity at a suitable level so as to balance between exploration and exploitation QAOA. This framework works for non-Markovian quantum systems with an arbitrary spectrum such that it is potentially easy to work on NISQ devices, thus paving the way for efficiently addressing tough combinatorial optimization problems.

-
- [1] P. Shor, Algorithms for quantum computation: discrete logarithms and factoring, in *Proceedings 35th Annual Symposium on Foundations of Computer Science* (1994) pp. 124–134.
- [2] P. Shor, Polynomial-time algorithms for prime factorization and discrete logarithms on a quantum computer, *SIAM Review*, **41**, 303 (1999).
- [3] L. K. Grover, A fast quantum mechanical algorithm for database search, in *Proceedings of the Twenty-Eighth Annual ACM Symposium on Theory of Computing* (1996) p. 212–219.
- [4] E. Farhi, J. Goldstone, and S. Gutmann, A quantum approximate optimization algorithm, *arXiv preprint arXiv:1411.4028*, (2014).
- [5] A. Callison and N. Chancellor, Hybrid quantum-classical algorithms in the noisy intermediate-scale quantum era and beyond, *Phys. Rev. A*, **106**, 010101 (2022).
- [6] E. Farhi, J. Goldstone, and S. Gutmann, A quantum approximate optimization algorithm applied to a bounded occurrence constraint problem, *arXiv: Quantum Physics*, (2014).
- [7] E. Farhi, Quantum supremacy through the quantum approximate optimization algorithm, *Bulletin of the American Physical Society*, **62** (2017).
- [8] A. B. Magann, K. M. Rudinger, M. D. Grace, and M. Sarovar, Feedback-based quantum optimization, *arXiv preprint arXiv:2103.08619* (2021).
- [9] S. Hadfield, Z. Wang, E. G. Rieffel, B. O’Gorman, D. Venturelli, and R. Biswas, Quantum approximate optimization with hard and soft constraints, in *Proceedings of the Second International Workshop on Post Moores Era Supercomputing* (2017) pp. 15–21.
- [10] S. Hadfield, Z. Wang, B. O’gorman, E. G. Rieffel, D. Venturelli, and R. Biswas, From the quantum approximate optimization algorithm to a quantum alternating operator ansatz, *Algorithms*, **12**, 34 (2019).
- [11] M. Willsch, D. Willsch, F. Jin, H. De Raedt, and K. Michielsen, Benchmarking the quantum approximate optimization algorithm, *Quantum Information Processing*, **19**, 1 (2020).
- [12] W. W. Ho and T. H. Hsieh, Efficient unitary preparation of non-trivial quantum states, *ArXiv e-prints*, (1803).
- [13] W. W. Ho, C. Jonay, and T. H. Hsieh, Ultrafast state preparation via the quantum approximate optimization algorithm with long range interactions, *arXiv preprint arXiv:1810.04817*, **11** (2018).
- [14] A. Frisk Kockum, D. Fitzek, M. Granath, T. Ghandriz, and L. Laine, Applying quantum approximate optimization to the heterogeneous vehicle routing problem, *Bulletin of the American Physical Society*, (2022).
- [15] M. Fingerhuth, T. Babej, and C. Ing, A quantum alternating operator ansatz with hard and soft constraints for lattice protein folding, *arXiv: Quantum Physics*, (2018).
- [16] J. S. Otterbach, R. Manenti, N. Alidoust, A. Bestwick, M. Block, B. Bloom, S. Caldwell, N. Didier,

- E. S. Fried, S. Hong, *et al.*, Unsupervised machine learning on a hybrid quantum computer, *arXiv preprint arXiv:1712.05771*, (2017).
- [17] A. Bengtsson, P. Vikstål, C. Warren, M. Svensson, X. Gu, A. F. Kockum, P. Krantz, C. Krizan, D. Shiri, I.-M. Svensson, *et al.*, Improved success probability with greater circuit depth for the quantum approximate optimization algorithm, *Phys. Rev. Appl.*, **14**, 034010 (2020).
- [18] D. Abrams, N. Didier, B. Johnson, M. Da Silva, and C. Ryan, Implementation of the XY interaction family by calibration of a single pulse, *Bulletin of the American Physical Society*, **65** (2020).
- [19] M. P. Harrigan, K. J. Sung, M. Neeley, K. J. Satzinger, F. Arute, K. Arya, J. Atalaya, J. C. Bardin, R. Barends, S. Boixo, *et al.*, Quantum approximate optimization of non-planar graph problems on a planar superconducting processor, *Nature Physics*, **17**, 332 (2021).
- [20] G. Pagano, A. Bapat, P. Becker, K. S. Collins, A. De, P. W. Hess, H. B. Kaplan, A. Kyprianidis, W. L. Tan, C. Baldwin, *et al.*, Quantum approximate optimization of the long-range ising model with a trapped-ion quantum simulator, *Proceedings of the National Academy of Sciences*, **117**, 25396 (2020).
- [21] L. Zhou, S.-T. Wang, S. Choi, H. Pichler, and M. D. Lukin, Quantum approximate optimization algorithm: Performance, mechanism, and implementation on near-term devices, *Phys. Rev. X*, **10**, 021067 (2020).
- [22] Z. Jiang, E. G. Rieffel, and Z. Wang, Near-optimal quantum circuit for grover's unstructured search using a transverse field, *Phys. Rev. A*, **95**, 062317 (2017).
- [23] M. B. Hastings, Classical and quantum bounded depth approximation algorithms, *arXiv preprint arXiv:1905.07047*, (2019).
- [24] Z. Wang, S. Hadfield, Z. Jiang, and E. G. Rieffel, Quantum approximate optimization algorithm for Maxcut: A fermionic view, *Phys. Rev. A*, **97**, 022304 (2018).
- [25] J. M. Larkin, M. Jonsson, D. Justice, and G. G. Guerreschi, Evaluation of QAOA based on the approximation ratio of individual samples, *Quantum Science and Technology*, (2022).
- [26] S. Bravyi, A. Kliesch, R. Koenig, and E. Tang, Obstacles to variational quantum optimization from symmetry protection, *Phys. Rev. Lett.*, **125**, 260505 (2020).
- [27] P. C. Lotshaw, T. S. Humble, R. Herrman, J. Ostrowski, and G. Siopsis, Empirical performance bounds for quantum approximate optimization, *Quantum Information Processing*, **20** (2021).
- [28] J. Preskill, Quantum Computing in the NISQ era and beyond, *Quantum*, **2**, 79 (2018).
- [29] Y. Pan, Y. F. Tong, S. Xue, and G. F. Zhang, Efficient depth selection for the implementation of noisy quantum approximate optimization algorithm, *arXiv:2207.04263v1* (2022).
- [30] L. C. Venuti, D. D'Alessandro, and D. A. Lidar, Optimal control for closed and open system quantum optimization, *arXiv preprint arXiv:2107.03517*, (2021).
- [31] Z.-C. Yang, A. Rahmani, A. Shabani, H. Neven, and C. Chamon, Optimizing variational quantum algorithms using pontryagin's minimum principle, *Phys. Rev. X*, **7**, 021027 (2017).
- [32] M. Mahdianand H. D. Yeganeh, Incoherent quantum algorithm dynamics of an open system with near-term devices, *Quantum Information Processing*, **19**, 1 (2020).
- [33] Z. Liu, L.-M. Duan, and D.-L. Deng, Solving quantum master equations with deep quantum neural networks, *Phys. Rev. Res.*, **4**, 013097 (2022).
- [34] J. Chen and H. I. Nurdin, Learning nonlinear input-output maps with dissipative quantum systems, *Quantum Information Processing*, **18**, 1 (2019).
- [35] P. Nimbe, B. A. Weyori, and A. F. Adekoya, Models in quantum computing: a systematic review, *Quantum Information Processing*, **20**, 1 (2021).
- [36] S. Xue, L. Tan, R. Wu, M. Jiang, and I. R. Petersen, Inverse-system method for identification of damping-rate functions in non-Markovian quantum systems, *Phys. Rev. A*, **102**, 042227 (2020).
- [37] L. Tan, D. Dong, D. Li, and S. Xue, Quantum Hamiltonian identification with classical colored measurement noise, *IEEE Transactions on Control Systems Technology*, **29**, 1356 (2020).
- [38] S. Xue, J. Zhang, and I. R. Petersen, Identification of non-Markovian environments for spin chains, *IEEE Transactions on Control Systems Technology*, **27**, 2574 (2019).
- [39] A. Lucas, Ising formulations of many NP problems, *Frontiers in Physics*, **2**, 5 (2014).
- [40] K. Bharti, A. Cervera-Lierta, T. H. Kyaw, T. Haug, S. Alperin-Lea, A. Anand, M. Degroote, H. Heimonen, J. S. Kottmann, T. Menke, *et al.*, Noisy intermediate-scale quantum algorithms, *Reviews of Modern Physics*, **94**, 015004 (2022).
- [41] Q. Wang and T. Abdullah, An introduction to quantum optimization approximation algorithm (2018).
- [42] H. Breuer and F. Petruccione, *The Theory of Open Quantum Systems* (OUP Oxford, 2007).
- [43] S. Xue, T. Nguyen, M. R. James, A. Shabani, V. Ugrirovskii, and I. R. Petersen, Modeling for non-Markovian quantum systems, *IEEE Transactions on Control Systems Technology*, **28**, 2564 (2019).
- [44] C. Gardiner, P. Zoller, and P. Zoller, *Quantum noise: a handbook of Markovian and non-Markovian quantum stochastic methods with applications to quantum optics* (Springer Science & Business Media, 2004).
- [45] L. Bouten, R. Van Handel, and M. James, An introduction to quantum filtering, *SIAM Journal on Control and Optimization*, **46**, 2199 (2007).
- [46] G. Burkard, Non-markovian qubit dynamics in the presence of $1/f$ noise, *Phys. Rev. B*, **79**, 125317 (2009).
- [47] L. Chirolli and G. Burkard, Decoherence in solid-state qubits, *Advances in Physics* **57**, 225 (2008).
- [48] S.-B. Xue, R.-B. Wu, W.-M. Zhang, J. Zhang, C.-W. Li, and T.-J. Tarn, Decoherence suppression via non-markovian coherent feedback control, *Phys. Rev. A* **86**, 052304 (2012).
- [49] S. Xue, M. R. Hush, and I. R. Petersen, Feedback tracking control of non-markovian quantum systems, *IEEE Transactions on Control Systems Technology* **25**, 1552 (2017).
- [50] S. Xue, T. Nguyen, M. R. James, A. Shabani, V. Ugrirovskii, and I. R. Petersen, Modelling and filtering for non-markovian quantum systems, *arXiv preprint arXiv:1704.00986*, (2017).
- [51] K. P. Murphy, *Machine learning: a probabilistic perspective* (MIT Press, 2012).
- [52] H.-P. Breuer, E.-M. Laine, and J. Piilo, Measure for the degree of non-Markovian behavior of quantum processes in open systems, *Phys. Rev. Lett.*, **103**, 210401 (2009).

- [53] M. Coggan, Exploration and exploitation in reinforcement learning, *Research supervised by Prof. Doina Precup, CRA-W DMP Project at McGill University*, (2004).